

# Dynamic carotid plaque imaging using ultrasonography

Argyrios A. Giannopoulos, PhD,<sup>a,b</sup> Efthymoulos Kyriacou, PhD,<sup>c</sup> Maura Griffin, PhD,<sup>d</sup> Constantinos S. Pattichis, PhD,<sup>e</sup> Joanna Michael, BSc,<sup>b</sup> Toby Richards, FRCS,<sup>b,f</sup> George Geroulakos, PhD,<sup>a,g</sup> and Andrew N. Nicolaides, PhD (Hon),<sup>d,h</sup> *London, United Kingdom; Lemesos and Nicosia, Cyprus; Crawley, Western Australia, Australia; and Athens, Greece*

## ABSTRACT

**Objective:** Dynamic image analysis of carotid plaques has demonstrated that during systole and early diastole, all plaque components will move in the same direction (concordant motion) in some plaques. However, in others, different parts of the plaque will move in different directions (discordant motion). The aim of our study was (1) to determine the prevalence of discordant motion in symptomatic and asymptomatic plaques, (2) to develop a measurement of the severity of discordant motion, and (3) to determine the correlation between the severity of discordant motion and symptom prevalence.

**Methods:** A total of 200 patients with 204 plaques resulting in 50% to 99% stenosis (112 asymptomatic and 92 symptomatic plaques) had video recordings available of the plaque motion during 10 cardiac cycles. Video tracking was performed using Farneback's method, which relies on frame comparisons. In our study, these were performed at 0.1-second intervals. The maximum angular spread (MAS) of the motion vectors at 10-pixel intervals in the plaque area was measured in degrees. Plaques were classified as concordant (MAS, <70°), moderately discordant (MAS, 70°-120°), and discordant (MAS, >120°).

**Results:** Motion was discordant in 89.1% of the symptomatic plaques but only in 17.9% of asymptomatic plaques ( $P < .001$ ). The prevalence of symptoms increased with increasing MAS. For a MAS >120°, the hazard ratio for the presence of symptoms was 47.7 (95% confidence interval, 18.1-125.6) compared with the rest of the plaques after adjustment for the degree of stenosis and mean pixel motion. The area under the receiver operating characteristic curve for the prediction of the presence of symptoms using the MAS was 0.876 (95% confidence interval, 0.823-0.929). The use of the median MAS (120°) as a cutoff point classified 86% of the plaques correctly (sensitivity, 81.4%; specificity, 91.2%; positive predictive value, 90.2%; and negative predictive value, 83.0%).

**Conclusions:** The use of the MAS value to identify asymptomatic plaques at increased risk of developing symptoms and, in particular, stroke should be tested in prospective studies. (*J Vasc Surg* 2021;73:1630-8.)

**Keywords:** Atherosclerotic carotid plaque; Concordant; Discordant; Motion analysis; Ultrasound

Intervention for carotid artery disease is routinely determined by the degree of internal carotid artery stenosis and the presence of recent symptoms. However, a proportion of patients with asymptomatic carotid plaques could have a high risk of future stroke.<sup>1</sup> In contrast, those with recent symptoms might have a low risk.<sup>2</sup> With advances in imaging methods, significant efforts have ensued to identify the vulnerable carotid plaque using, not only the degree of stenosis, but also the plaque texture features on computed tomography,<sup>3</sup> magnetic resonance imaging (MRI),<sup>4</sup> and/or ultrasonography.<sup>5</sup>

Ultrasonography remains the most commonly used imaging modality to evaluate for carotid artery disease and

provides information on the degree of stenosis and morphology of the carotid plaque. The ACSRS (asymptomatic carotid stenosis and risk of stroke) study followed up 1121 patients with 50% to 99% internal carotid artery stenosis for a mean of 4 years (range, 6 months to 8 years).<sup>1,6</sup> That study showed that, after image normalization, a number of plaque texture features such as a low gray scale median, the presence of a large juxtaluminal black area without a visible echogenic cap, or the presence of discrete white areas in a hypoechoic region were associated with an increased stroke risk. It also showed that the combination of these texture features with the degree of stenosis and the presence or absence of a history of

From the Department of Vascular Surgery, Faculty of Medicine, Imperial College London, London<sup>a</sup>; the Department of Vascular Surgery, University College London Hospital, London<sup>b</sup>; the Department of Electrical and Computer Engineering and Informatics, Frederick University, Lemesos<sup>c</sup>; the Vascular Screening and Diagnostic Centre, Nicosia<sup>d</sup>; the Department of Computer Science, University of Cyprus, Nicosia<sup>e</sup>; the Division of Surgery, University of Western Australia, Crawley<sup>f</sup>; the Department of Vascular Surgery, Attikon Hospital, National and Kapodistrian University of Athens, Athens<sup>g</sup>; and the Department of Vascular Surgery, University of Nicosia Medical School, Nicosia.<sup>h</sup>

Author conflict of interest: none.

Correspondence: Argyrios A. Giannopoulos, PhD, Department of Vascular Surgery, Faculty of Medicine, Imperial College London, Exhibition Rd, London, UK SW7 2BU (e-mail: [a.giannopoulos13@alumni.imperial.ac.uk](mailto:a.giannopoulos13@alumni.imperial.ac.uk)).

The editors and reviewers of this article have no relevant financial relationships to disclose per the JVS policy that requires reviewers to decline review of any manuscript for which they may have a conflict of interest.

0741-5214

Copyright © 2020 by the Society for Vascular Surgery. Published by Elsevier Inc.

<https://doi.org/10.1016/j.jvs.2020.10.021>

contralateral symptoms could stratify patients into different stroke risk categories ranging from 0.5% to 14% annually.<sup>1,6</sup> However, one third of the strokes had occurred in the low-risk group, suggesting that other causes of plaque rupture could be present.<sup>1,6</sup>

Improvements in the resolution of B-mode ultrasonography enabled the assessment of dynamic plaque motion during the cardiac cycle and the measurement of deformability (strain) of carotid plaques. Pilot studies have suggested that echolucent plaques or echolucent areas of heterogeneous plaques will demonstrate greater deformability than will echogenic plaques or echogenic areas of heterogeneous plaques.<sup>7-9</sup> Comparative studies of carotid plaques assessed as high risk using MRI had increased maximum motion on ultrasound elastography (peak strain) compared with stable plaques.<sup>10</sup>

Internal stress is the force responsible for plaque rupture when it exceeds a certain value (yield stress), which cannot be measured using ultrasound scans. However, a marker of increased stress can be derived from the presence of motion (strain) in different directions that occurs in the plaque. The ability to do this with ultrasonography was first demonstrated by Meairs and Hennerici<sup>11</sup> in 1999. They showed that asymptomatic plaques had surface motion vectors of equal orientation and magnitude to those of the internal carotid artery wall.<sup>11</sup> However, symptomatic plaques had inherent surface movements that differed in magnitude and direction from the carotid wall.<sup>11</sup>

Our team, and others, have subsequently demonstrated that the observations by Meairs and Hennerici<sup>11</sup> apply to the whole area of the two-dimensional longitudinal B-mode image of carotid bifurcation plaques.<sup>9,12-14</sup> In some plaques, the motion of all plaque components will be in the same direction and magnitude (concordant motion). However, in others, different parts of the plaque will demonstrate motion in different directions and magnitude (discordant motion).<sup>15,16</sup>

Our hypothesis was that discordant motion would be an indication of high plaque internal stress and that the quantitation of this discordant motion would be an indirect measurement of the severity of the risk of plaque rupture and, by inference, the risk of symptoms developing. The aim of our study was (1) to determine the prevalence of discordant motion in symptomatic and asymptomatic plaques, (2) to develop a measurement of the severity of discordant motion, and (3) to determine the association of discordant motion and absolute motion (irrespective of the direction) with the presence of symptoms.

## METHODS

**Patients.** Patients who had undergone ultrasound imaging for symptomatic and asymptomatic carotid artery stenosis >50% in relation to the lumen of the normal

## ARTICLE HIGHLIGHTS

- **Type of Research:** A multicenter, prospective, cross-sectional study
- **Key Findings:** Pixel motion was measured in 112 asymptomatic and 92 symptomatic carotid plaques from cine loops obtained using B-mode ultrasonography. An increased maximum angular spread of vectors was strongly related to the presence of discordant motion and symptom prevalence. A cut-off point of 120° classified 86% of the plaques correctly as symptomatic or asymptomatic.
- **Take Home Message:** The results from the present study suggest a practical and reliable method of studying carotid plaque motion that can be used in the identification of high-risk plaques prone to rupture.

distal internal carotid artery (NASCET [North American Symptomatic Carotid Endarterectomy Trial] method) were recruited. These patients had undergone evaluation at three different vascular laboratories at University College London Hospital, Ealing Hospital, and the Vascular Screening and Diagnostic Centre (London, United Kingdom). The London-Harrow national research ethics service committee approved the present study (approval no. 11/LO/0299), and the included patients provided written informed consent.

**Clinical information.** The clinical information collected was primarily the presence or absence of a transient ischemic attack or stroke in relation to the hemispheric cerebral side as diagnosed by the referring neurologist or surgeon. Age, gender, systolic and diastolic blood pressure (BP), and the degree of internal carotid stenosis were recorded. Hypertension was considered present if the systolic BP was >140 mm Hg or diastolic BP >90 mm Hg or the patient was receiving antihypertensive therapy.

**Grading of internal carotid stenosis.** A combination of velocity criteria and velocity ratios were used to express the degree of stenosis in relation to the diameter of the distal internal carotid (NASCET method).<sup>15</sup> The Philips iU22 ultrasound system (Philips Ultrasound, Bothell, Wash) with an L9-3 linear array probe was used.

**Image capture of plaque motion.** At the end of the routine carotid duplex ultrasound scan, video recording of the B-mode images of the plaque was performed initially with color flow or power Doppler to highlight the outline of the plaque and, subsequently, in gray scale for ~10 cardiac cycles. The ultrasound beam was at right angles to the arterial wall. The depth was minimal, usually 2 to 3 cm, such that the plaque would occupy a large part of the image. Gain was reduced to abolish noise and

then gradually increased to allow for a minimum of noise in the vessel lumen. During the recording, the patient was asked to stop breathing to prevent motion artifacts. The video recordings were anonymized and processed blindly.

**Video processing.** Video processing was performed with the user-friendly carotid plaque-motion analysis dedicated research software, as previously described.<sup>15,16</sup> This software estimates motion using Farneback's method,<sup>16</sup> which depends on frame comparisons. Initially, the color flow video was loaded and viewed to visualize the outline of the plaque. Next, the gray scale video was loaded (Fig 1, A, top left window). The software automatically detected the frame rate, shown in a window below the image. A point in the common carotid artery was selected (Fig 1, A and B, top left window, red dotted line), where the adventitia was bright and well delineated. This enabled the software to produce a well-defined M-mode image of the arterial wall (Fig 1, A and B, top right window), which was used subsequently for identification of systole and diastole. Next, the scale was defined using the centimeter markers on the right side of the image to allow the expression of all measurements on the image in millimeters. Subsequently, the operator outlined the plaque as the region of interest shown in red (Fig 1, A and B) and entered the number of frames per 0.1 second to allow frame comparisons for this standard time. Comparisons of the frames at 0.1-second intervals throughout the video were performed by the software. An arbitrary threshold of 0.08 mm was set to allow motion at less than this threshold, considered "noise," to be ignored. The results of frame comparisons were visualized by moving the cursor at the appropriate point on the M-mode image and saved in the patient's folder. A total of 6 to 15 comparisons (mean, 10 comparisons) performed during systole or early diastole when the plaque motion was maximum ( $>0.20$  mm) were saved. For each frame comparison selected, three new displays were provided: (1) the plaque image with green vectors spaced at 10-pixel intervals representing the magnitude of motion and direction (Fig 1, A and B, bottom left); (2) the directional motion distribution in a circular histogram with a column for each  $6^\circ$  angle (Fig 1, A and B, bottom middle); and (3) a scatterplot of the median pixel movement against the angle (Fig 1, A and B, bottom right).

**Measurements.** The first display (Fig 1, A and B, bottom left) provided a method of visual assessment of the presence of concordant or discordant motion. The second display (Fig 1, A and B, bottom middle) provided a method of determining the maximum angular spread (MAS) in degrees for pixel motions that were 20% of the peak motion (peak motion shown by the  $6^\circ$  arc that has the largest group of moving pixels). The third display (Fig 1,

A and B, bottom right) was a scatterplot of the median motion of all the pixels on the vertical axis against the angular spread for each frame comparison on the horizontal axis. This display enabled the calculation of the maximum median motion in millimeters (ie, the median of the pixel motions in the tallest column of the circular histogram) and the mean pixel motion of all the pixels in millimeters and its standard deviation (SD), irrespective of direction. These calculated measurements were displayed in three windows below the scattergram (Fig 1, A and B). Frame comparisons with a maximum motion of  $<0.20$  mm were ignored by the operator because such motion was considered to be less than the ultrasound resolution. The displays of each frame comparison were saved in an image folder. The calculated values were saved in a text file that can be opened in Excel (Microsoft, Redmond, Wash) and used to calculate the mean values of all frame comparisons for each plaque.

**Visual classification.** The plaques were classified visually into three groups according to the pixel motion during systole or early diastole: those with concordant motion (Fig 1, A), those with discordant motion (Fig 1, B), and those with moderate discordant motion. Concordant motion was considered present if all pixels in the plaque image moved in the same direction during systole in all cardiac cycles. Discordant motion was considered present if pixels moved in different directions (angle  $>45^\circ$ ) in  $>50\%$  of cardiac cycles. Moderate discordant motion was considered present if the pixels moved in different directions in  $<50\%$  of cardiac cycles.

Motion analysis of all the plaques ( $n = 204$ ) was performed twice by one person who was unaware of symptom status 1 month apart to determine intraobserver reproducibility. Of the 204 plaques, 59 (29%) from the first 59 recruited patients were also analyzed by a second person who was also unaware of symptom status to obtain interobserver reproducibility.

**Statistical analysis.** The prevalence of symptomatic plaques in relation to age, gender, degree of stenosis, and hypertension was explored using the  $\chi^2$  test. Because the prevalence of symptoms increased with lesions producing  $>80\%$  stenosis, the plaques were reclassified into two stenosis groups: 50% to 79% and 80% to 99%. Subsequently, the results of the two visual analyses performed by the same person and the analyses performed by the two different persons were compared using the kappa statistic. The prevalence of different types of plaque motion in the asymptomatic and symptomatic plaques and the prevalence of symptoms in the different plaque motion classes were determined. The  $\chi^2$  test was used to determine statistical significance.

The prevalence of symptomatic plaques using the quartiles of MAS, maximum median motion, mean pixel motion, and its SD was calculated. Because the

distribution of these continuous variables was not normal and because the change in prevalence across quartiles was not linear, the significant variables were reclassified. The MAS was divided into two groups using the median value ( $120^\circ$ ) as a cutoff point, and the mean pixel motion and its SD was divided into three groups by combining the third and fourth quartiles.

Subsequently, a multivariable linear logistic regression analysis was performed using symptom status (present vs absent) as the dependent variable and the reclassified measurements, including stenosis, as the explanatory variables. The developed logistic regression model was then used to calculate the risk of symptoms present for every plaque.

The receiver operating characteristic (ROC) curves were produced for the independent predictors for symptom presence. Using the optimum cutoff points (highest sensitivity combined with highest specificity) for the variables with the greatest areas under the ROC curve, a final plaque classification was produced.

## RESULTS

A total of 200 patients with 204 plaques with 50% to 99% stenosis (112 asymptomatic and 92 symptomatic plaques) were included in the present study. Of the 92 patients with symptomatic plaques, 29 had presented with carotid territory ipsilateral hemispheric carotid stroke and 63 with transient ischemic attacks, as determined by the referring physician. Other demographic data were as follows: age,  $73.0 \pm 9.5$  years; internal carotid stenosis,  $67.4\% \pm 13.6\%$ ; male gender, 64%; hypertension, 71%; smoking history, 38%; statin therapy, 67%; and antiplatelet therapy, 74%.

No statistical significance was found in the prevalence of symptoms in relation to age (<60, 60-70, 70-80, >80 years), gender, or hypertension. However, the prevalence of symptomatic plaques was greater in lesions with >80% stenosis. The prevalence of symptomatic plaques was 57.1% in patients with 80% to 99% and 41.3% in patients with 50% to 79% stenosis ( $P = .037$ ; odds ratio, 1.95; 95% confidence interval [CI], 1.04-3.79).

The intraobserver variability in the 204 plaques was high (kappa statistic, 0.843;  $P < .001$ ), and the interobserver variability in 59 plaques was good (kappa statistic, 0.736;  $P < .001$ ). The overall plaque motion was concordant in 75 plaques (36.8%), moderately discordant in 27 (13.2%), and discordant in 102 (50.0%; Table I). In symptomatic carotid plaques, the motion was discordant in 89.1% compared with only 17.9% in asymptomatic plaques with discordant motion ( $P < .001$ ; Table I).

The prevalence of symptoms was 2.7% in the presence of concordant motion, 29% in the presence of moderate discordant motion, and 80.4% in the presence of discordant motion ( $P < .001$ ). The prevalence of symptoms increased with an increasing MAS ( $P < .001$ ) but not with the maximum median motion ( $P = .233$ ; Table II).

The prevalence of symptoms decreased with increasing mean pixel motion ( $P < .001$ ) and its SD ( $P = .011$ ; Table II).

In a multivariable linear logistic regression analysis with symptom status (present vs absent) as the dependent variable and MAS, stenosis, maximum median motion, mean pixel motion, and SD of the mean pixel motion as explanatory variables, only the maximum angular motion, stenosis, and mean pixel motion were independent predictors of symptom presence (Table III). It can be seen from this model that the most important variable was MAS, with a hazard ratio of 47.7 (95% CI, 18.13-125.6) after adjustment for stenosis and mean pixel motion.

The relationships between MAS, mean pixel motion, plaque motion class, and symptom status are shown in Fig 2, A and B. The areas under the ROC curves of the significant variables for predicting the probability of the model for identifying the presence of symptoms were 0.876 (95% CI, 0.823-0.929) for MAS, 0.575 (95% CI, 0.496-0.655) for stenosis, and 0.285 (95% CI, 0.264-0.414) for mean pixel motion. The area under the ROC curve for the predicted probability for the presence of symptoms by the model was 0.917 (95% CI, 0.879-0.955), close to that for the MAS. Using 0.6 as the cutoff point of the predicted probability (highest sensitivity with the highest specificity), plaques could be classified into symptomatic or asymptomatic, with an accuracy of 86.3%. The use of the median MAS value ( $120^\circ$ ) as a cutoff point to classify plaques provided the same accuracy (Table IV). The prevalence of symptomatic plaques increased in relation to both stenosis (<80% or >80%) and MAS quartiles.

## DISCUSSION

The results of the present study have indicated that most symptomatic plaques (89.1%) will have inherent discordant motion in contrast to asymptomatic plaques, of which approximately only one sixth (17.9%) had discordant motion ( $P < .001$ ; Table I). This finding confirmed that high internal stresses are more common in symptomatic plaques.

Each green motion vector superimposed on the plaque image (Fig 1, A and B) showed the resultant motion per unit time (0.1 second in our study) for several movements: (1) the overall movement of the plaque with the arterial wall; and (2) the movement within the plaque. If the internal movement of different parts of the plaque were negligible or were all in the same direction, the resultant vectors will be in the same direction, indicating concordant motion. However, if the motions of different parts of the plaque were in different directions, the resultant vectors representing different pixels will no longer be parallel but will be at an angle. The MAS of the vectors is a measure of the spread of the directions of internal motion and, by inference, internal plaque stress. When internal motions are in near opposite directions, the MAS will be  $\geq 180^\circ$  (Fig 1, B). Our data have demonstrated that with an increasing MAS, an associated increase will

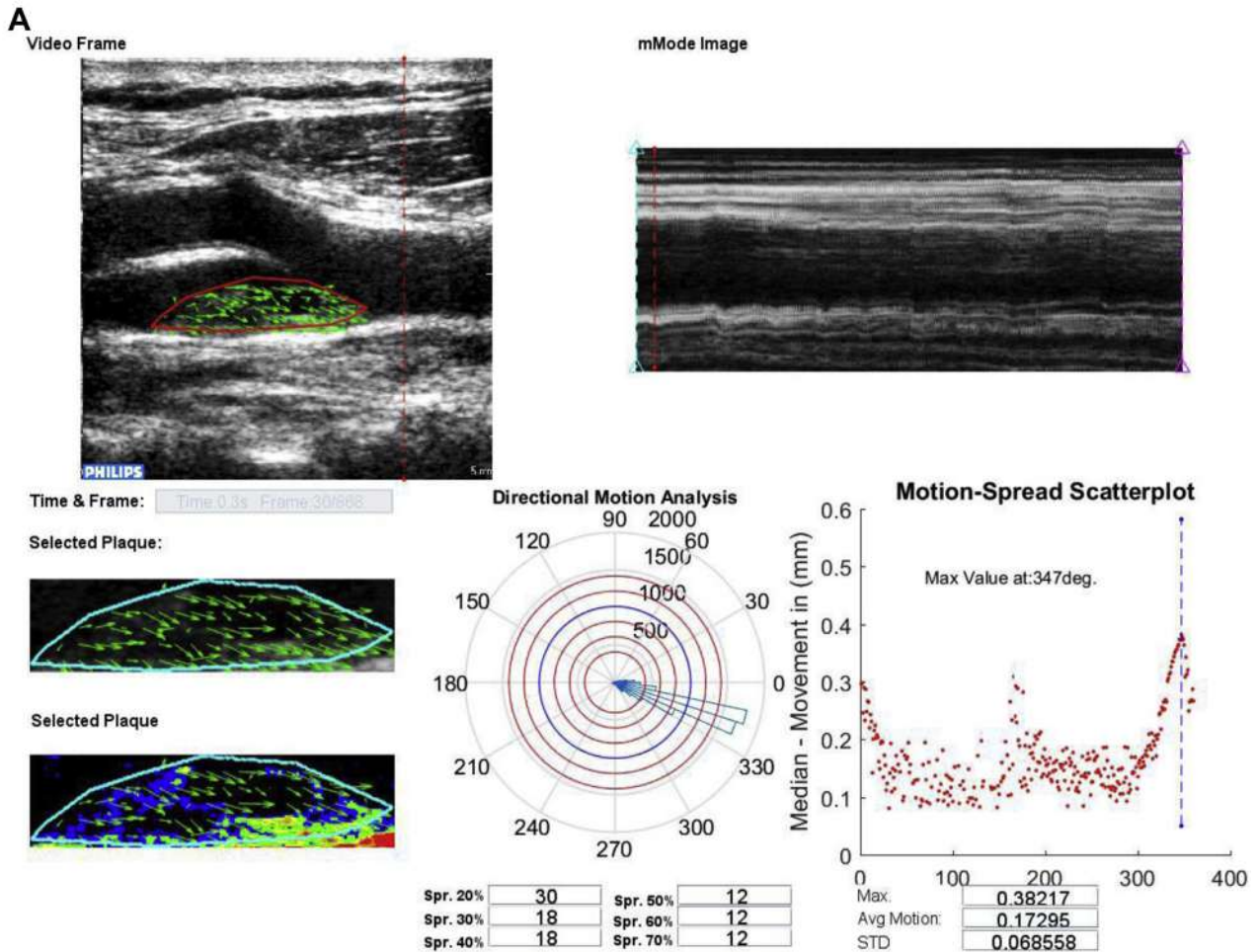


**Fig 1. A**, Plaque with concordant motion, with all pixels moving in the same direction during systole. The maximum angle between vectors was  $30^\circ$  at a maximum pixel motion of 0.38 mm. **B**, Plaque with discordant motion, with pixels moving in different directions during systole. The maximum angle between vectors was  $162^\circ$  at a maximum pixel motion of 0.31 mm.

occur in the prevalence of symptomatic plaques (Table II). MAS values of  $<70^\circ$  were associated with plaques visually classified as having concordant motion, intermediate MAS values of  $70^\circ$  to  $120^\circ$  with moderate discordant motion, and MAS values  $>120^\circ$  with discordant motion (Fig 2, A). Also, MAS values  $>120^\circ$  were associated with predominantly symptomatic plaques (Fig 2, B). This finding supports our hypothesis that MAS, a computer-generated continuous variable, is a quantitative measure of the severity of discordant motion and a marker of plaque instability.

The association between the low mean pixel motion and high prevalence of symptoms or discordant motion (Table II) is difficult to explain. It might result from different opposing forces (ie, high MAS) reducing the overall plaque motion. However, compared with the MAS, it had a relatively small contribution to the diagnostic strength of the multivariable logistic model (Table III).

The prevalence of symptomatic plaques also increased with stenosis  $>80\%$ , indicating the presence of a patient selection bias. The adjustment for the severity of stenosis was achieved in the multivariable linear logistic model, confirming the statistical significance of MAS (Table III).

Theoretical calculations of the internal stresses (forces) of the plaques using MRI geometry and two-dimensional fluid structure interaction modelling in recent studies suggested that symptomatic plaques had greater stress than asymptomatic plaques. The calculated higher stress in the symptomatic plaques was associated with the presence of a greater lumen curvature and were independent of the degree of luminal stenosis or plaque composition.<sup>17-19</sup> These findings support the belief that it is the combination of inherent structure weakness and dynamic stress that exceeds the yield stress that results in plaque rupture.

In our present study, the orientation of two-dimensional pixel motion of the whole plaque area

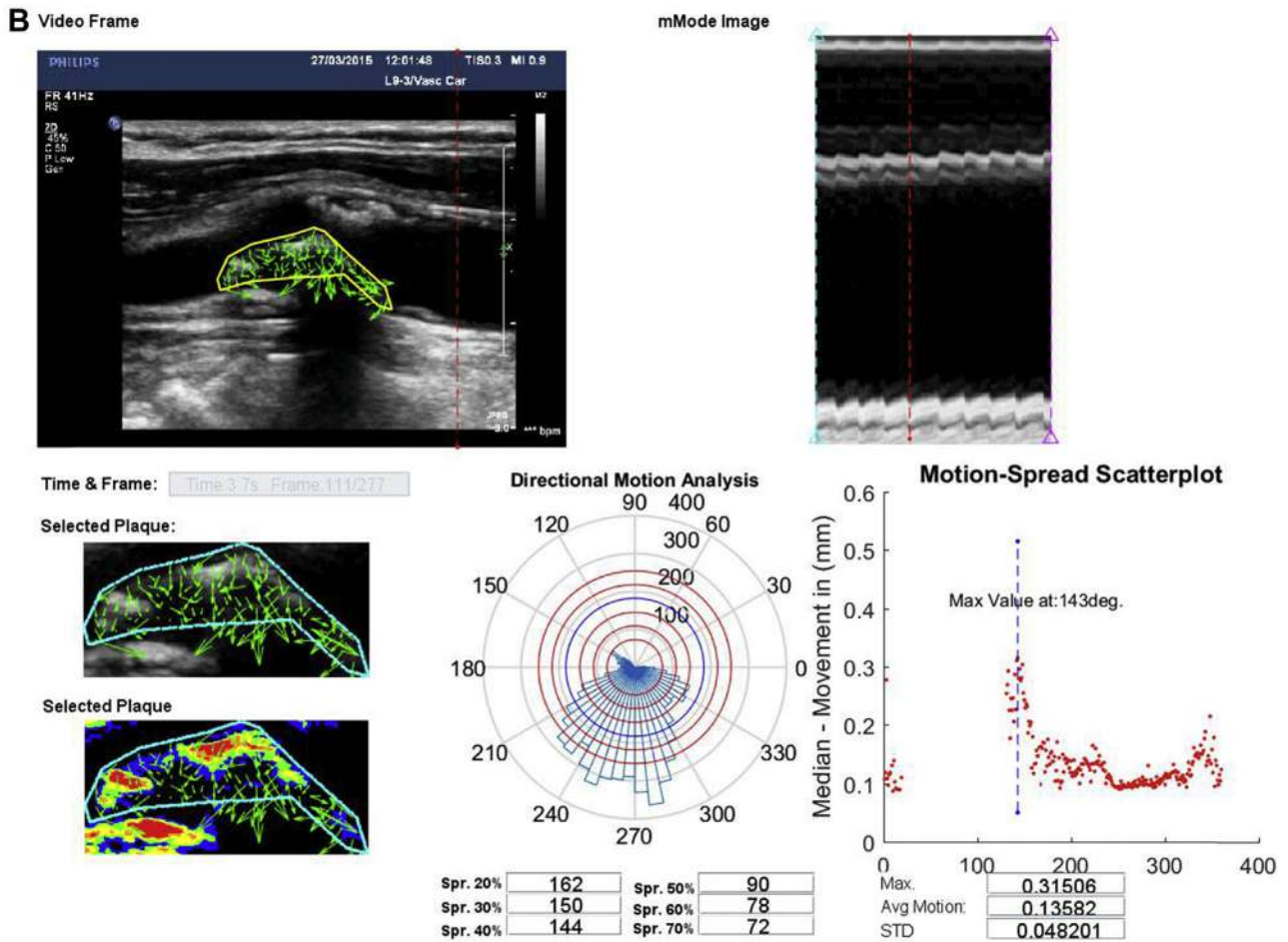


Fig 1. Continued.

with its quantitation provided by the MAS was used to measure the plaque internal stress. The MAS is the end product of the external pressure forces on the plaque during the cardiac cycle combined with plaque consistency, geometry, and inherent weakness of the plaque body and fibrous cap.

Several forces are responsible for the motion of the different plaque components. Just before systolic flow, the pulse pressure wave that travels fast along the arterial tree results in a rapidly increasing pressure, followed by a slower decrease in pressure during diastole. The pulse pressure has already been demonstrated to be a strong independent predictor of ulceration of symptomatic carotid plaques.<sup>20</sup> Increased velocity in the stenosis during systole is associated with increased shear stress and a decrease in pressure along the stenosis; thus, the plaque is subjected to a high pressure proximally and a reduced pressure distally.<sup>21</sup> A further local reduction in pressure within the stenosis can be produced by the Bernoulli effect, which can result in a paradoxical reduction of the lumen cross-sectional area during systole.<sup>22-24</sup> Turbulence and vibrations by a bruit will result in additional

stress on the plaque.<sup>25</sup> Thus, different parts of the plaque will be subjected to different forces that can be calculated or measured in laboratory models but not in vivo.<sup>25</sup> However, the resultant motions (strain) of different parts of the plaque can be detected by video recordings of B-mode ultrasonography. Their directions and magnitudes are an indication of the stresses within the plaque. Future studies are required to investigate the association between the peak systolic and end-diastolic velocities with MAS.

Our method of measuring MAS is reproducible and practical. The recording of the video at the end of the routine carotid examination is within the capability of all ultrasonographers, adds very little time to the whole procedure, and has already been shown to be practical in an established vascular laboratory performing routine carotid scans.<sup>9</sup> The use of dedicated software specifically written by one of us (E.K.) allows for the motion estimations to be performed using a laptop computer within <20 minutes.

One limitation of the study was that the design was cross-sectional. However, because the results have

**Table I.** Prevalence of plaque motion classes stratified by symptom status ( $P < .001$ ;  $\chi^2$  test)

Symptom status	Plaque motion			Total
	C	MD	D	
Asymptomatic	73 (65.2)	19 (17.0)	20 (17.9)	112 (100)
Symptomatic	2 (2.2)	8 (8.7)	82 (89.1)	92 (100)
Total	75 (36.8)	27 (13.2)	102 (50.0)	204 (100)

C, Concordant; D, discordant; MD, moderately discordant.

**Table II.** Prevalence of symptomatic plaques and odds ratios for quartiles of maximum angular spread, maximum median motion, mean pixel motion, and standard deviation

Variable	Range	Plaques, No.	Symptomatic, No. (%)	Unadjusted OR (95% CI)	P value for trend ( $\chi^2$ )
MAS quartile, °					<.001
First	<53	51	2 (3.9)	1	
Second	53-121	51	7 (13.7)	3.90 (0.69-19.7)	
Third	121-186	51	44 (86.3)	154 (30.3-780)	
Fourth	>186	51	39 (76.5)	79.6 (16.8-376)	
MMM quartile, mm					.233
First	<0.2803	51	26 (51)	1	
Second	0.2803-0.3346	51	27 (52.9)	1.08 (0.50-2.35)	
Third	0.3346-0.4302	51	18 (35.3)	0.52 (0.24-1.16)	
Fourth	>0.4302	51	21 (41.2)	0.67 (0.31-1.47)	
MPM quartile, mm					<.001
First	<0.1359	51	39 (76.5)	1	
Second	0.1359-0.1568	51	25 (49.0)	0.29 (0.13-0.69)	
Third	0.1568-0.1896	51	15 (29.4)	0.13 (0.05-0.31)	
Fourth	>0.1896	51	13 (25.5)	0.10 (0.04-0.26)	
SD quartile, mm					.011
First	<0.0367	51	32 (62.7)	1	
Second	0.0367-0.0494	51	24 (47.1)	0.53 (0.24-1.16)	
Third	0.0494-0.0663	51	20 (39.2)	0.38 (0.17-0.85)	
Fourth	>0.0663	51	16 (31.4)	0.27 (0.12-0.62)	

CI, Confidence interval; MAS, maximum angular spread; MMM, maximum median motion; MPM, mean pixel motion; OR, odds ratio; SD, standard deviation.

**Table III.** Multivariable linear logistic regression with symptom status as dependent variable<sup>a</sup>

Variable	HR	95% CI	P value
MAS ( $\leq 120^\circ$ vs $> 120^\circ$ )	47.72	18.13-125.6	<.001
Stenosis ( $< 80\%$ vs $\geq 80\%$ )	4.074	1.288-12.89	.017
Mean pixel motion ( $< 0.1359$ mm, $0.1359$ - $0.1568$ mm, vs $> 0.1568$ mm)	0.470	0.276-0.801	.005
Constant	0.043	NA	<.001

CI, Confidence interval; HR, hazard ratio; MAS, maximum angular spread; NA, not applicable.  
<sup>a</sup>Maximum angular spread, stenosis, and mean pixel motion were the only significant explanatory variables.

demonstrated that 17.9% of the asymptomatic plaques exhibited discordant movement and because concordant movement was rarely found in symptomatic plaques, our observations led to a new hypothesis that asymptomatic plaques with discordant movement are

the ones most likely to become symptomatic. This new hypothesis requires testing in a prospective study of patients with asymptomatic carotid stenosis receiving optimal medical therapy. Additionally, the plaque texture features already established as indicators of

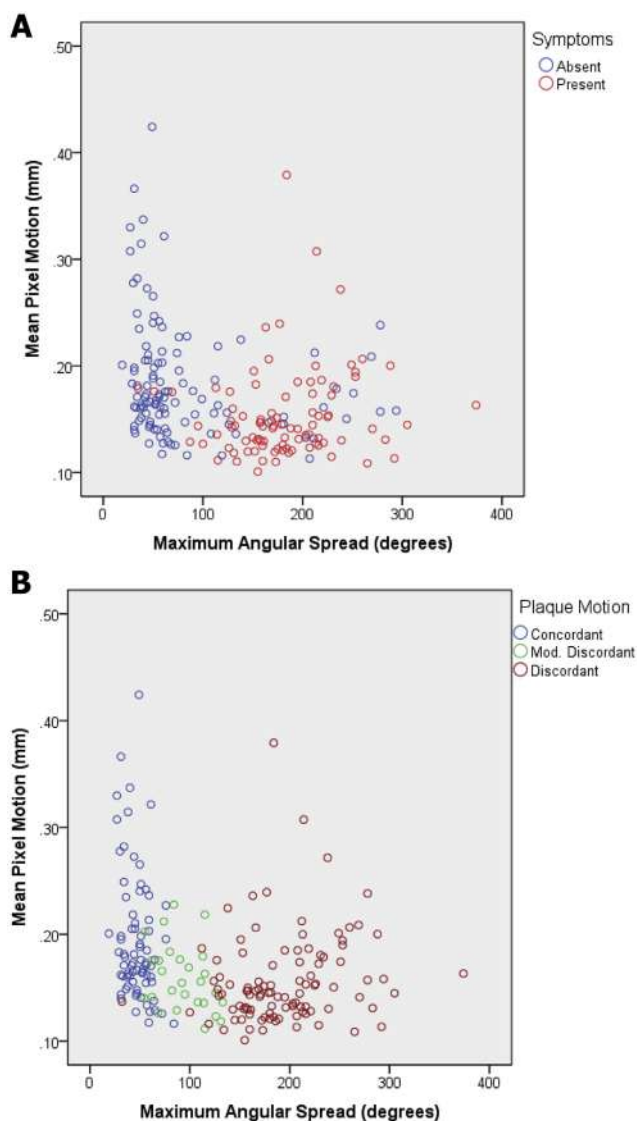


**Fig 2. A,** Relationship between maximum angular spread, mean pixel motion, and plaque motion class. **B,** Relationship between maximum angular spread, mean pixel motion, and the presence or absence of symptoms.

increased stroke risk could also be studied such that one could determine whether the discordant movement is an independent predictor of stroke risk and whether, when combined with plaque texture features, will result in more accurate stroke risk stratification.

### CONCLUSIONS

Carotid plaque motion analysis of cine loops obtained using B-mode ultrasonography is now practical and can be performed using a laptop computer. Discordant motion is an indication of high plaque internal stress, and quantitation of this discordant motion by measuring the angular spread of motion vectors is an indirect measurement of the severity of the risk of plaque rupture and, by inference, the risk of symptoms developing. The

**Table IV.** Classification of plaques using logistic regression model of maximum angular spread<sup>a</sup>

Plaque classification using logistic model or MAS	Clinical symptom status, No. (%)		Total, No.
	Absent	Present	
Predicted as asymptomatic or MAS $\leq 120^\circ$	93 (91.2)	9 (8.8)	102
Predicted as symptomatic or MAS $>120^\circ$	19 (18.6)	83 (81.4)	102
Total	112 (54.9)	92 (45.1)	204

MAS, Maximum angular spread.  
<sup>a</sup>Median MAS of  $120^\circ$  as cutoff point ( $P < .001$ ,  $\chi^2$  test); sensitivity, 81.4%; specificity, 91.2%; positive predictive value, 90.2%; negative predictive value, 83.0%; overall accuracy, 86.3%; false-positive result, 17.0%; and false-negative result, 9.8%.

prevalence of discordant motion was 89.1% in the symptomatic and 17.9% in the asymptomatic plaques. The angular spread of motion vectors is a measurement of the severity of discordant motion and associated with increasing symptom prevalence. It should be used in prospective studies of asymptomatic carotid plaques to determine its ability to predict for symptom development.

### AUTHOR CONTRIBUTIONS

Conception and design: AG, EK, MG, CP, GG, AN  
 Analysis and interpretation: AG, EK, MG, TR, GG, AN  
 Data collection: AG, MG, JM, AN  
 Writing the article: AG, EK, TR, AN  
 Critical revision of the article: AG, EK, MG, CP, JM, TR, GG, AN  
 Final approval of the article: AG, EK, MG, CP, JM, TR, GG, AN  
 Statistical analysis: AG, MG, AN  
 Obtained funding: Not applicable  
 Overall responsibility: AG

### REFERENCES

- Nicolaidis AN, Kakkos SK, Kyriacou E, Griffin M, Sabetai M, Thomas DJ, et al: Asymptomatic Carotid Stenosis and Risk of Stroke (ACRS) Study Group. Asymptomatic internal carotid artery stenosis and cerebrovascular risk stratification. *J Vasc Surg* 2010;52:1486-96.
- Rothwell PM, Warlow CP. Prediction of benefit from carotid endarterectomy in individual patients: a risk-modelling study. European Carotid Surgery Trialists' Collaborative Group. *Lancet* 1999;353:2105-10.
- de Weert TT, Cretier S, Groen HC, Homburg P, Cakir H, Wentzel JJ, et al. Atherosclerotic plaque surface morphology in the carotid bifurcation assessed with multidetector computed tomography angiography. *Stroke* 2009;40:1334-40.
- Schindler A, Schinner R, Altaf N, Hosseini AA, Simpson RJ, Esposito-Bauer L, et al. Prediction of stroke risk by detection of hemorrhage in carotid plaques: meta-analysis of individual patient data. *JACC Cardiovasc Imaging* 2020;13:395-406.
- Griffin MB, Kyriacou E, Pattichis C, Bond D, Kakkos SK, Sabetai M, et al. Juxtaluminal hypoechoic area in ultrasonic images of carotid plaques and hemispheric symptoms. *J Vasc Surg* 2010;52:69-76.

6. Kakkos SK, Griffin MB, Nicolaides AN, Kyriacou E, Sabetai MM, Tegos T, et al: Asymptomatic Carotid Stenosis and Risk of Stroke (ACRS) Study Group. The size of juxtaluminal hypoechoic area in ultrasound images of asymptomatic carotid plaques predicts the occurrence of stroke. *J Vasc Surg* 2013;57:609-18.
7. Widman E, Caidahl K, Heyde B, D'hooge J, Larsson M. Ultrasound speckle tracking strain estimation of in vivo carotid artery plaque with in vitro sonometry validation. *Ultrasound Med Biol* 2015;41:77-88.
8. Liu F, Yong Q, Zhang Q, Liu P, Yang Y. Real time tissue elastography for the detection of vulnerable carotid plaques in patients undergoing endarterectomy: a pilot study. *Ultrasound Med Biol* 2015;41:705-12.
9. Khan AA, Siddhartha S, Hatsukami T, Cebra J, Jones M, Huston J, et al. Noninvasive characterization of carotid plaque strain. *J Vasc Surg* 2017;65:1653-63.
10. Huang C, Pan X, He Q, Huang M, Huang L, Zhao X, et al. Ultrasound-based carotid elastography for detection of vulnerable atherosclerotic plaques validated by magnetic resonance imaging. *Ultrasound Med Biol* 2016;42:367-77.
11. Meairs S, Hennericci M. Four-dimensional ultrasonographic characterization of plaque surface motion in patients with symptomatic and asymptomatic carotid artery stenosis. *Stroke* 1999;30:1807-13.
12. Nasrabadi H, Pattichis MS, Fisher P, Nicolaides AN, Griffin M, Makris GC, et al. Measurement of motion of carotid bifurcation plaques. 2012 IEEE 12th International Conference on Bioinformatics and Bioengineering; pp 506-511. Available at: <https://ieeexplore.ieee.org/document/639972>. Accessed February 20, 2020.
13. Kyriacou E, Nicolaides A, Griffin M, Constantinou A, Loizou CP, Pattichis M, et al. Carotid bifurcation plaque stability estimation based on motion analysis. Proceedings of the 30th IEEE International Symposium on Computer Based Medical Systems June 22-24, 2017, Thessaloniki, Greece. Available at: <https://doi.org/10.1109/CBMS.2017.52>. Accessed February 20, 2020.
14. Stoitsis J, Colemati S, Nikita KS, Nicolaides AN. Characterization of carotid atherosclerosis based on motion and texture features and clustering using fuzzy c-means. *Conf Proc IEEE Eng Med Biol Soc* 2004;2004:1407-10.
15. Nicolaides AN, Shifrin EC, Bradbury A, Dhanjil S, Griffin M, Belcaro G, et al. Angiographic and duplex grading of internal carotid stenosis: can we overcome the confusion? *J Endovasc Surg* 1996;3:158-65.
16. Farneback G. Polynomial expansion for orientation and motion estimation. PhD Thesis. Linköping, Sweden: Linköping University; 2002.
17. Trivedi RA, Li ZY, U-King-Im J, Graves MJ, Kilpatrick PJ, Gillard JH. Identifying vulnerable carotid plaques in vivo using high resolution magnetic resonance imaging-based finite element analysis. *J Neurosurg* 2007;107:536-42.
18. Gao H, Long Q. Effects of varied lipid core volume and fibrous cap thickness on stress distribution in carotid arterial plaques. *J Biomech* 2008;41:3053-9.
19. Li ZY, Tang T, U-King-Im J, Graves M, Sutcliffe M, Gillard JH. Assessment of carotid plaque vulnerability using structural and geometrical determinants. *Circ J* 2008;72:1092-9.
20. Lovett IK, Howard SC, Rothwell PM. Pulse pressure is independently associated with carotid plaque ulceration. *J Hypertens* 2003;21:1669-76.
21. Imbesi SG, Kerber CW. Why do ulcerated atherosclerotic carotid artery plaques embolize? A flow dynamics study. *AJR Am J Neuroradiol* 1998;19:761-6.
22. Beach KW, Hatsukami T, Detmer P, Primozich JF, Ferguson MS, Gordon D, et al. Carotid artery intraplaque haemorrhage and stenotic velocity. *Stroke* 1993;24:314-9.
23. Lal BK, Beach KW, Sumner DS. Intracranial collateralization determines hemodynamic forces for carotid plaque disruption. *J Vasc Surg* 2011;54:1461-71.
24. Xu C, Yuan C, Stutzman E, Canton G, Comess KA, Beach KW. Quest for the vulnerable atheroma: carotid stenosis and diametric strain-a feasibility study. *Ultrasound Med Biol* 2016;42:699-716.
25. Zouggari L, Bou-said B, Massi F, Culla A, Millon A. The role of biomechanics in the assessment of carotid atherosclerosis severity: a numerical approach. *World J Vasc Surg* 2018;1:1-8.

Submitted May 12, 2020; accepted Oct 3, 2020.